A Molecular Beam Study of the NO + CO Reaction on Pd(111) Surfaces

Kandasamy Thirunavukkarasu,[†] Krishnan Thirumoorthy,[†] Jörg Libuda,[‡] and Chinnakonda S. Gopinath*[,†]

Catalysis Division, National Chemical Laboratory, Dr. Homi Bhabha Road, Pune 411 008, India, and Department of Chemical Physics, Fritz-Haber-Institut der Max-Planck-Gesellschaft, Faradayweg 4−6, 14195 Berlin, Germany

Received: January 27, 2005; In Final Form: May 6, 2005

Nitric oxide (NO) reduction with carbon monoxide (CO) on the Pd(111) surface was studied under isothermal conditions by molecular beam techniques as a function of temperature, NO:CO beam composition, and beam flux. Systematic experiments were performed under transient and steady state conditions. Displacement of adsorbed CO by NO in the transient state of the reaction was observed at temperatures between 375 and 475 K for all the NO:CO compositions studied. NO accumulation occurs on Pd(111) surface under steady state conditions, below 475 K, due to stronger chemisorption of NO. The steady state reaction rates attain a maximum at about 475 K, nearly independent of beam composition. N_2 was found to be the major product of the reduction, along with a minor production of N_2O. The production of N_2 and N_2O indicates molecular and dissociative adsorption of NO on Pd(111) at temperatures up to 525 K. Postreaction TPD measurements were performed in order to determine the nitrogen coverage under steady-state conditions. Finally, the results are discussed with respect to the rate-controlling character of the different elementary steps of the reaction system.

1. Introduction

The importance of the catalytic removal of nitrogen oxides (NO_x) from exhaust gases, is well documented.[1−3] NO_x leads to acid rains, creation of ozone at the ground level, and other severe environmental problems. Regulations for the control of NO_x emissions in automobiles have dramatically increased all over the world, stimulating extensive research on this topic.[1−3] The automobile exhaust and the stationary power generation centers are the main sources for NO_x pollution in the atmosphere. For the past few years, three-way catalytic (TWC) converters in the automobiles have employed Pd in addition to other active metals (Pt, Rh) for emission control through oxidation of CO and hydrocarbons to CO_2 and reduction of NO_x to N_2. However, problems arise under oxidizing atmospheres and the increasing costs of the precious metals is also a concern.[4] Although the overall NO + CO reaction in TWC is known, a complete microscopic understanding of the elementary reaction steps is not yet in place, especially for Pd. Further, NO_x reduction performance at low temperatures and resistance to oxidation of the metal particles at high temperatures has led to an increased interest in Pd.[5] Recent reports on Pd−CeO_2 and Pd−Rh−CeO_2 show similar or even superior catalytic performance over the conventional Rh−Pt−CeO_2.[6] Other than the above, a few new technologies were introduced in the past decade such as NO_x storage and zeolite based catalysts in order to tackle NO_x abatement.[7−9] Nonetheless, stability problems associated with NO_x storage and the inability of zeolites to cause NO reduction in the presence of water vapor[10] are problems faced in real applications.

A number of groups[11−31] have studied deNO_x reactions with CO or H_2 as the reductant on Pd single crystals, Pd on supports, and powder catalysts. Still, the kinetics of the reaction is not fully understood. Infrared reflection−absorption spectroscopy (IRAS) and high-resolution electron energy loss spectroscopy (HREELS) have been employed to study NO adsorption and its coadsorption with CO on Pd(100) and Pd(111) single crystals.[20,21] Goodman and co-workers found that the closely packed Pd(111) surface was significantly more active than the relatively more open Pd(100) surface for the NO + CO reaction,[20,21] although the latter has a higher NO dissociation activity. This effect was attributed to the strong bonding of a fraction of the N_{ads} on Pd(100), leading to partial poisoning of the surface.[20] Also, the N_2/N_2O product ratio was found to depend on the crystallographic orientation, with lower selectivity for N_2 on Pd(111) than on Pd(100). In more recent work, high N_2O/N_2 product ratios were observed on the Pd(111) surface at elevated pressures.[21] Some differences remain between the TPD results reported by Goodman et al.[20] on Pd(111) and Pd(100) and those reported by other groups,[13,22,28−31] in particular, with respect to N_2 desorption above 550 K.

Well-shaped Pd nanoclusters supported on MgO, with Pd-(111) and Pd(100) facets, were employed in NO dissociation studies by Henry et al.[23−25] Relatively high reaction rates were observed on Pd(111) facets, in good agreement with ref 20. Particle size dependent effects were interpreted mainly in terms of the morphology of the particles, which expose different fractions of (111) and (100) facets.[23−25] Recent microkinetic simulations of the molecular beam experiments show that there are many open questions concerning the reaction kinetics, even for simple single-crystal surfaces.[25] From the above it is clear that there is a need for detailed and quantitative kinetic measurements on Pd single-crystal surfaces under well-controlled conditions.

* Corresponding author. E-mail: cs.gopinath@ncl.res.in. Fax: 0091-20-2589 3761.
[†] National Chemical Laboratory.
[‡] Fritz-Haber-Institut der Max-Planck-Gesellschaft.

10.1021/jp050478v CCC: $30.25
Published on Web 06/21/2005

The present work on the NO + CO reaction on Pd(111) is a part of our continuing study of NO reduction reactions in our laboratory.[31] The reactivity of Pd(111) surfaces for NO + CO reactions at different temperatures and beam compositions have been investigated systematically. We have employed molecular beam methods, which have enabled us to perform kinetic experiments in a quantitative and well-controlled fashion, both under steady state and under transient conditions. In this paper, we present results on the reaction kinetics at low and high temperatures and on the competitive adsorption of NO and CO at temperatures between 375 and 475 K.

2. Experimental Section

All molecular beam and TPD experiments reported here were performed in a homemade 12 L capacity stainless steel ultrahigh vacuum (UHV) chamber evacuated with a turbo-molecular drag pump to a base pressure of 3×10^{-10} Torr. This system is equipped with a quadrupole mass spectrometer (Pfeiffer QMS 200 M3) for the detection of all the relevant gas-phase species of the reaction, a sputtering ion gun for cleaning the sample and a molecular beam doser for beam generation. The QMS is placed out of line-of-sight to avoid any angular effect that might arise from single crystals. More details of our experimental setup along with NO/Pd(111) results may be found in ref 31. Briefly, the doser assembly, aiming directly at the crystal surface, is connected to a gas manifold unit and the beam flux is set both by filling the manifold unit to a specified pressure and by fixing the precision leak valve to a predetermined position. Here 0.1 ML/s total flux of the NO + CO mixture (F_{NO+CO}) with a desired composition was used in all the experiments reported here unless otherwise specified. A movable stainless steel shutter is placed between the sample and the doser to block or unblock the beam when desired. The geometrical arrangement in our MBI is such that about 25% of the beam is intercepted by the crystal, and hence, the drop in the reactants pressure upon shutter removal is relatively shallow; this is mainly to ensure a uniform beam profile over the entire crystal surface.[31]

A circular disk of Pd(111) single crystal, 8 mm in diameter, was mounted by spot-welding a tantalum wire (0.5 mm thick) to the periphery of the crystal and the temperature is measured by a chromel−alumel thermocouple, spot-welded to the backside of the crystal. The crystal can be resistively heated to 1200 K, and cooled to 120 K with liquid nitrogen, controlled through a homemade temperature controller. The Pd(111) sample was cleaned by Ar^+ sputtering in the presence of an oxygen atmosphere (oxygen pressure of 5×10^{-8} Torr, total pressure of 1×10^{-6} Torr) at 1000 K and subsequent flashing to 1200 K. The procedure was repeated until no CO and CO_2 were observed in subsequent TPD spectra recorded after oxygen adsorption.[28] The cleanliness of the Pd(111) surface was further checked by AES and XPS in another UHV chamber. There were no Si, S, and P impurities detected on Pd(111). ^{15}NO (Air gas, 99% isotopically pure), CO, and ^{13}CO (Isotec) were used without any further purification. It is to be noted that ^{15}NO contains about 1% of ^{14}NO (amu 30), which adds to the partial pressure of $^{15}N_2$ (amu 30) during measurements. Very small amount of $^{15}N_2O$ (amu 46) ($\leq$0.1%) is also present; however, it does not affect the measurements since the amount is very small. However, ^{15}NO allows a clear identification of all the products of the reaction $^{15}N_2$ (amu 30), $^{15}N_2O$ (amu 46), and $^{12}CO_2$ (amu 44) along with the reactants, ^{15}NO (amu 31) and ^{12}CO (amu 28). It is observed that N_2O gives a key fragment ion N_2 to a large extent. The partial pressure values observed during the reaction for N_2O and N_2 were corrected for the above fragment contribution by following the procedure in ref 32. The mass spectrometer intensities for ^{15}NO and CO were calibrated by measuring the NO and CO uptake on clean Pd(111) at 300 K separately, assuming a saturation coverage of 0.33 monolayer (ML) for NO following Jacobi et al.[29] and 0.50 ML for CO.[33] An exposure of 1 ML corresponds to 7.8×10^{14} molecules/cm^2. ^{15}NO and CO were exclusively used for all the experiments reported here. Hence, hereafter ^{15}NO would be simply noted as NO. Further, the rates calculated and given in Figures 9, 10, and 12 have an error margin of $\pm$10%.

3. Results

3.1. General Aspects on Catalytic Activity Measurements. In all the isothermal experiments reported here, the clean Pd(111) sample was kept at a constant temperature and exposed to an effusive molecular beam of the reactant mixture of the desired composition. The partial pressures of all the relevant species were recorded as a function of time. A typical raw isothermal kinetic data of the reaction of ^{15}NO and CO with a beam composition of 1:2 at 475 K is presented in Figure 1a along with the TPD spectra recorded at a heating rate of 5 K/s (Figure 1b). The scattered data points for all the species were collected without opening the shutter in a separate experiment. The various steps in all the experiments are explained below with reference to the above data: (1) At $t = 5$ s a molecular beam of a mixture of the reactants (NO:CO = 1:2, F_{NO+CO} = 0.10 ML/s) was turned on; an immediate increase in NO and CO partial pressures could be seen. Some adsorption of the reactants from the "background" cannot be avoided at this stage. (2) At around $t = 8$ s the shutter was removed to allow the beam to interact directly with the Pd(111) surface kept at 475 K. An immediate decrease in the partial pressure of the reactants was observed indicating the adsorption of the reactants on the Pd(111) surface. A slow increase in NO partial pressure was due to decreasing adsorption on the UHV chamber walls and does not indicate a change in the F_{NO} on Pd(111). An increase in the partial pressure of the products, $^{15}N_2$ (30 amu), CO_2 (44 amu) and $^{15}N_2O$ (46 amu) were also observed. The changes observed from the point where the shutter is opened until the steady state is reached is termed as the transient state, and this normally takes up to 2 min under the present experimental conditions. (3) In the steady state, the reaction rate was measured by blocking the beam deliberately for 30 s (between $t = 165-195$ s) with the shutter. An increase in the partial pressure of NO and a clear decrease in the partial pressures of N_2 and CO_2 were observed. A slight decrease in the partial pressure of N_2O was also observed. An increase in the partial pressure of NO indicates its continuous uptake from the beam in the steady state; a sharp change in the CO partial pressure was observed only at the blocking and unblocking of the beam, but an overall increase was not observed during the beam blocking time. The measured changes in the partial pressures of CO_2, N_2, and N_2O allow us to directly determine the steady-state reaction rates. Additional kinetic information can be derived from the transient response (see section 3.2). A sharp decrease in the CO_2 partial pressure was observed when the beam was blocked, whereas a slow change in partial pressure was observed for the N_2 and N_2O. It is to be pointed out here that the change in the partial pressure of the reactants and the products has to be corrected for the background adsorption, during the period the beam was blocked in the steady state which is estimated to be around 10% for the adsorption processes in our system. (4) The shutter is opened again at $t = 195$ s. The pressure difference observed for the reactants and the products during beam blocking and unblocking

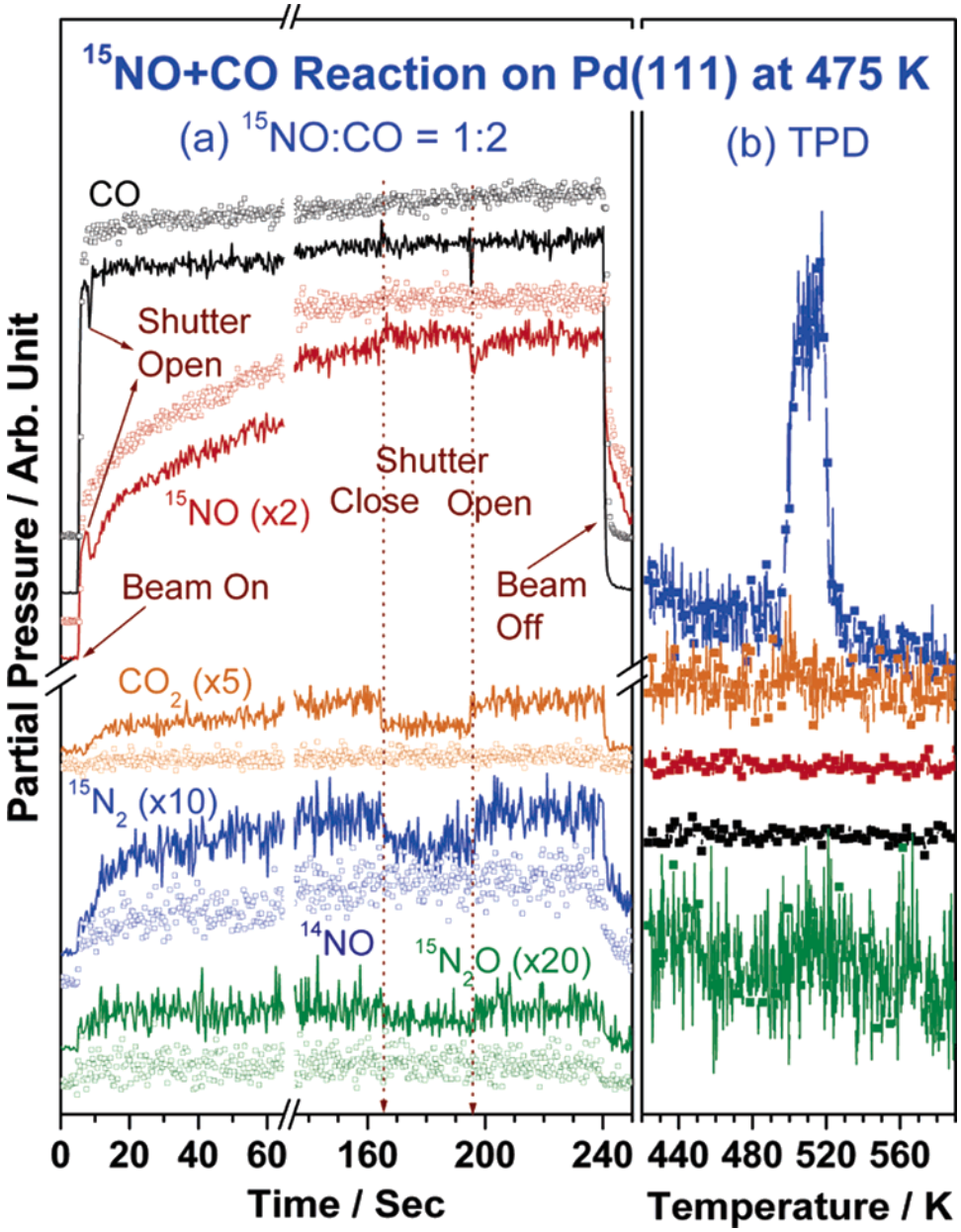

Figure 1. (a) Raw isothermal kinetic data of a typical molecular beam experiment conducted with (NO + CO)/Pd(111) system at 475 K for the beam composition of 1:2 NO:CO. (b) Temperature-programmed desorption recorded after the kinetic experiment. Scattered data points shown on left panel are from the experiment carried out without opening the shutter throughout the experiment to demonstrate the marginal effect due to background. Data points have been shifted vertically for clarity. An increase in amu 30 intensity in the above experiment is essentially due to ^{14}NO present in ^{15}NO.

provides the rate of the reaction, of course after initial calibration of all the relevant species. (5) At about $t = 240$ s, the beam was turned off to stop the reaction. After the pressure of the UHV chamber reached the initial background level, the sample was heated to 700 K at a heating rate of 5 K/s to record the TPD of all the relevant species. The coverage by the nitrogen atoms that remained on the Pd(111) surface was calculated by integrating the area of the N_2 desorption peak observed in the TPD, and oxygen coverage was measured through CO titration at 450 K. A systematic study of the NO + CO reaction kinetics on Pd(111) surfaces was carried out by following the above procedure as a function of temperature, NO:CO composition, and total beam flux.

During the reaction measurements, the total pressure in the chamber increases to about $(1-2) \times 10^{-8}$ Torr and that induces some additional adsorption/reaction apart from the direct beam onto Pd(111). As shown in Figure 1, the reactants pressure increase in the same manner, whether the beam was blocked or not, except while opening/closing the shutter. However, the products pressure increases marginally when the beam was fully blocked, as seen in the scattered data points due to the limited adsorption from the background. CO_2 shows an increase in pressure and displays that there is reaction to some extent due to background adsorption of NO + CO. In the case of $^{15}N_2$ (amu 30) a large increase in background pressure is mostly due to 1% ^{14}NO (amu 30), in addition to some $^{15}N_2$. Indeed, at low temperature (375 K) measurements, where there is no effective reaction, show a very similar trend and supports the above increase in pressure is due to ^{14}NO. It was difficult to make out any contribution due to the very poor signal/noise associated with the data of $^{15}N_2O$ production from background. However, at the time of shutter opening/closing, a good change in partial pressure of all the products demonstrate that major contribution is due to molecular beam. Further, the extent of CO_2 production

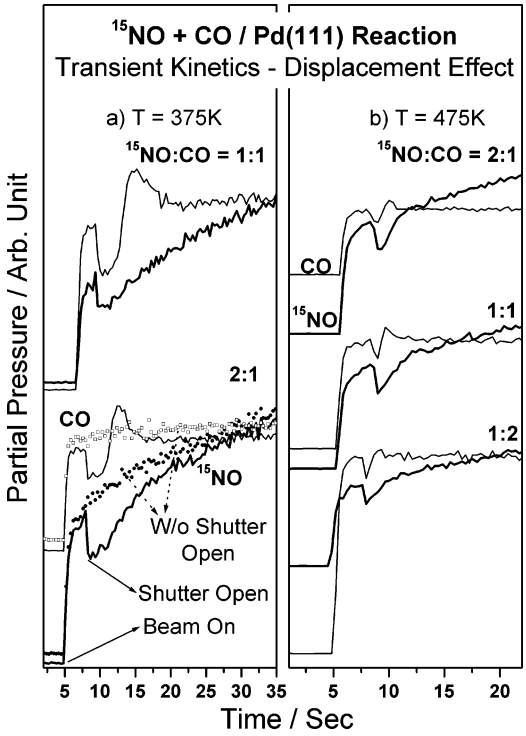

Figure 2. Displacement of CO by NO during the initial adsorption of the reactants on clean Pd(111) surface at (a) 375 and (b) 475 K for the NO:CO beam compositions 2:1, 1:1, and 1:2. The F_{NO+CO} used in panel b is twice that of panel a, and displacement effect was not clear at lower flux at 475 K. Scattered data points shown on left panel for 2:1 beam are from the experiment carried out without opening the shutter to use as standard for background subtraction. Similar experiments were carried out for other experiments.

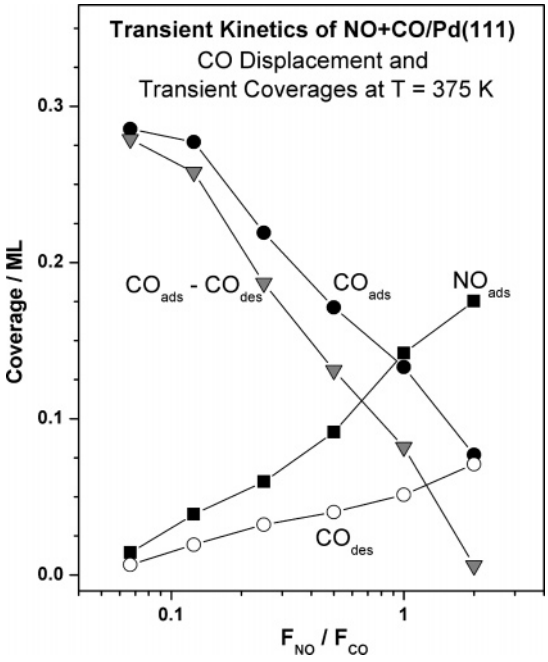

Figure 3. Coverage of NO and CO in the transient state on NO + CO (1:1)/Pd(111) system at 375 K. NO_{ads}, CO_{ads}, and CO_{des} correspond to the coverage of NO and CO immediately after shutter removal and coverage of desorbed CO in the transient state, respectively. The difference between $CO_{ads} - CO_{des}$ gives qualitative CO-coverage on the surface at the end of transient state. It is to be noted that the surface is increasingly poisoned by CO with CO-rich beams and an almost exclusively NO-covered surface occurs for a 2:1 NO:CO beam.

due to background adsorption is not more than 10% of the CO_2 produced from the direct beam. However, a similar measurement for $^{15}N_2$ was not reliable as the background is largely due to ^{14}NO. For the above reason, the background contribution is not included in the results reported. As shown in Figure 12 (vide infra) the partial pressure of different species were converted into reaction rates by calibration experiments for the reactants and products, following the procedure reported,[31] and no background contribution is included.

3.2. Transient Kinetics. First, we focus on the transient regime of the reaction, immediately after impingement of the beam. A clean metal surface at the start of the reaction undergoes dynamic changes in surface composition of reactants and products as a function of time before it reaches the steady state, where there is no change in surface composition of reactants as long as the reaction conditions are not perturbed. It is important to note that the sticking coefficients of the reactants NO and CO may drastically change as a function of temperature and coverage in the transient region.

3.2.1. Displacement of CO by NO. The displacement of a chemisorbed species by another adsorbing species has been suggested and observed by few groups[16,20,25,34] in various catalytic reactions. Figure 2 shows the direct displacement of CO_{ads} by NO at (a) 375 K and (b) 475 K for the NO:CO compositions of 2:1, 1:1, and 1:2. The F_{NO+CO} used in Figure 2b is (0.3 ML/S) thrice that used in the experiments of Figure 2a (0.1 ML/S). Reference experiments were also carried out without opening the shutter, and the data collected were used for background subtraction from the data of the relevant experiments. One such reference experiment is plotted in Figure 2a for 2:1 NO:CO beam composition. The trends of NO adsorption (Figure 2) follow the expected behavior at all the temperatures and compositions. An initial drop in the partial pressure is observed upon shutter removal due to initial uptake on Pd(111) and a subsequent asymptotic approach to the steady state. The time evolution of partial pressure of CO is more complex. An immediate drop in the partial pressure upon unblocking the beam was observed, followed by an increase in partial pressure after few seconds. Finally, the steady-state level is reached. It indicates that a large amount of CO is displaced by NO because of its preferential adsorption on Pd(111) compared to CO. This effect was observed for all beam compositions at 375 K. For CO-rich beam compositions the process is slower since the CO displacement is directly proportional to F_{NO}. Generally as the beam becomes richer in CO (and hence poor in NO), the displacement of CO molecules takes a longer time. It is also to be noted that the CO displacement effect decreased with decreasing F_{NO+CO}; the extent of CO displacement was marginal at a $F_{NO+CO} = 0.1$ ML/s at 475 K for the beam compositions shown in Figure 2b. At temperatures ≥ 525 K the displacement effect was very poor or not observed due to the very small steady state coverage of the reactants, particularly CO.[33] However at temperatures <525 K, this effect was observed clearly and the surface ratio of the reactants changed in the transient state until it reached the steady state. It is also clear from these observations that the adsorption of NO on Pd(111) is dominating and hence an enrichment of NO over CO occurs compared to the gas phase. A similar effect has already been observed on Rh(111).[34]

Figure 3 shows the coverages of NO_{ads}, CO_{ads}, and CO_{des} and the difference between CO_{ads} and CO_{des} on Pd(111) in the transient state for all the NO:CO compositions at 375 K. The above coverages were obtained by integrating the area of the adsorption and desorption in the transient state (Figure 2). NO_{ads} decreases linearly as the beam becomes CO-rich. Initial CO_{ads} also increases with the CO-rich beams. However the amount

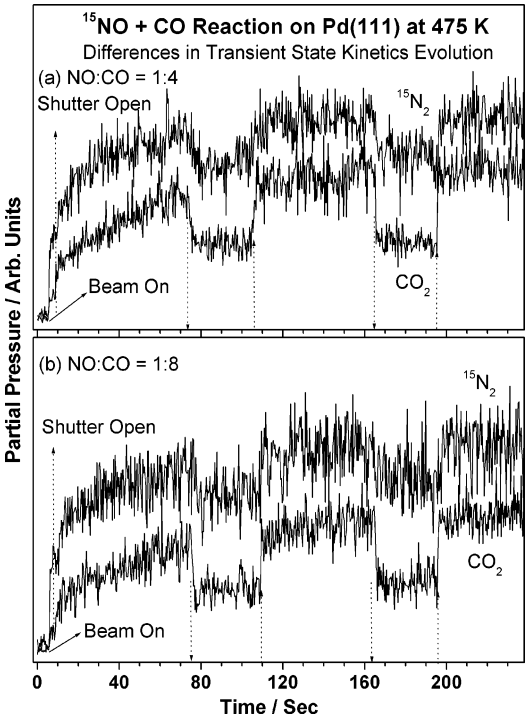

Figure 4. Time evolution of the partial pressure of the products $^{15}N_2$ and CO_2 in the transient state for NO:CO beam compositions of (a) 1:4 and (b) 1:8 at 475 K. It is to be noted that the partial pressure of CO_2 reaches steady-state slowly than N_2 and it is attributed, at least in part, to CO poisoning and CO displacement by NO. The change in CO_2 partial pressure for beam blocking is considerably lower in the transient state than in the steady state.

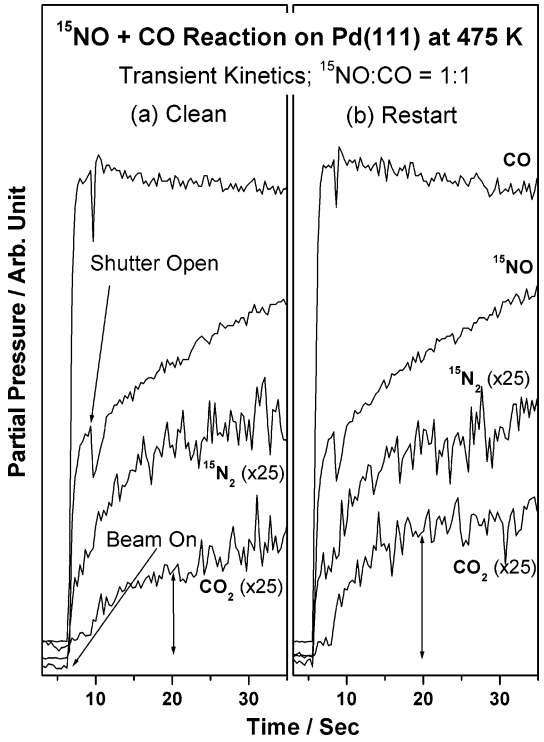

Figure 5. Isothermal kinetic experiments carried out with a 1:1 NO:CO beam at 475 K on (a) clean Pd(111) and (b) on the Pd-surface after reaction a, but without any cleaning. An enhancement in CO_2 production could be seen in the transient state indicates that some amount of oxygen available.

of CO_{des} indicates that the CO displacement is very strong for NO-rich beams and gradually decreases as the beam becomes richer in CO. Only minor CO-displacement was observed for 1:15 NO:CO beam. The present results reveal a clear difference between surface and beam compositions the surface accumulating NO.

Figure 4 shows the transient state kinetics of CO_2 and N_2 evolution at 475 K for two NO:CO compositions, namely, 1:4 and 1:8. CO_2 production shows a transient kinetics depending on NO:CO beam composition. At high F_{NO} (with 2:1 of NO:CO data not shown), the CO_2 production rate is low and it increases with increasing F_{CO} up to 1:4 NO:CO. A further increase in F_{CO} leads to a decrease in the CO_2 formation rate, likely due to CO poisoning of the surface. Generally, the N_2 production reaches the steady state within a minute; however the CO_2 production reaches the steady state slowly in about 2 min. This delay occurs especially with NO:CO compositions (1:1 to 1:8) that exhibit a high rate of CO_2 production. However such a delay does not occur with NO- or CO-rich beams since the CO displacement effect is observed too fast or too slow and hence the poisoning of the surface with NO or CO, respectively. With a 1:15 NO:CO composition, the CO_2 production reaches a steady-state quickly within 20 s after shutter removal and the rate is limited by CO-poisoning. A close look at the transient state in Figure 4 shows a jump in CO_2 production at the point of shutter opening and some delay in N_2 production. Further, the change in CO_2 partial pressure for beam blocking at $t = 75$ s shows a considerably smaller change in rate and a slower CO_2 decay when compared to the sharp changes at $t = 165$ s. However, the change in nitrogen partial pressure is similar at both beam blockings. We attribute this delay, at least in part, to the CO displacement effect and a continuous change in surface composition until it reached the steady-state. Nonetheless, the above observation has to be treated with care due to the low signal-to-noise ratio for the N_2 signal. A slower response of the N_2 signal would indicate that the N_2 recombination step has some significant degree of rate control. Spectroscopic and structural investigations could throw more light on the changes that might be occurring on the surface under reaction conditions.

3.2.2. Restart Experiments. Restart experiments were performed in order to identify differences in the transient state due to accumulation of surface species, produced during the reaction. Figure 5 shows such an example, where clean Pd(111) interacted with 1:1 NO:CO beam ($F_{NO+CO} = 0.25$ ML/s) for about 120 s (in Figure 5a) before the molecular beam was turned off. After the partial pressures of all the species reached their background level the reaction was repeated without any further cleaning of the Pd(111) surface and the result is shown in Figure 5b. A decrease in the partial pressure due to adsorption of NO and CO and the displacement effect in the transient state was observed on clean and restart experiments. The partial pressures for N_2 and N_2O increased to the steady state value gradually without any significant change in both the clean and restart experiments. However, a considerable increase in the CO_2 formation was observed in the restart experiments. Even before the shutter removal a small but considerable CO_2 production started as soon as the molecular beam was turned on due to the reaction of the background CO on the Pd(111) surface. After shutter removal, a further rise in the CO_2 production was observed compared to the clean surface. This immediate production of CO_2 was more pronounced for NO-rich beams. However, the rate of formation of CO_2 remained unchanged in the steady state for clean and restart experiments. The displacement of CO by NO also decreased significantly in the restart experiments. This effect is attributed to the additional CO_2 production due to reaction with surface oxygen in the restart experiment. CO_2 production was instantaneous in restart experi-

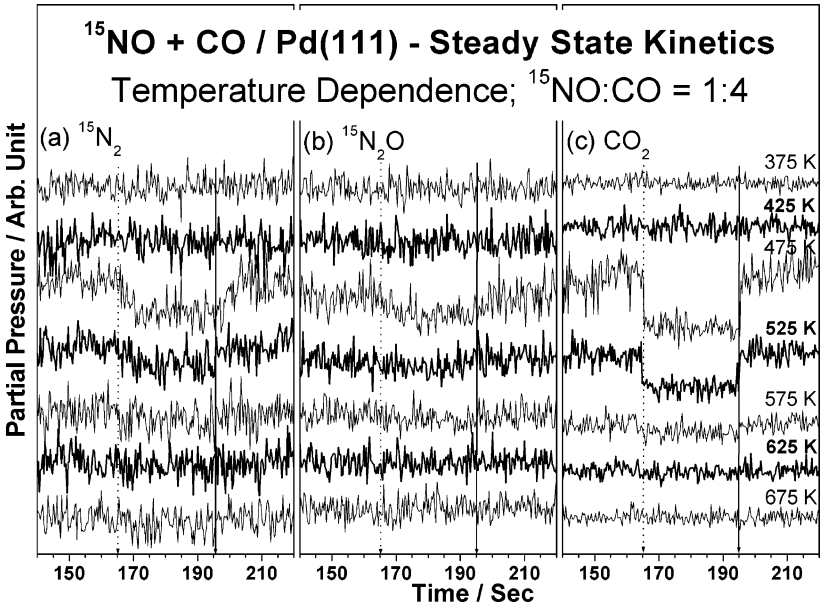

Figure 6. Steady-state kinetics of isothermal experiments as a function of temperature with a 1:4 NO:CO composition and time evolution of the partial pressure of the products (a) N_2, (b) N_2O, and (c) CO_2. Dotted and solid arrows indicate the closing and opening of the shutter.

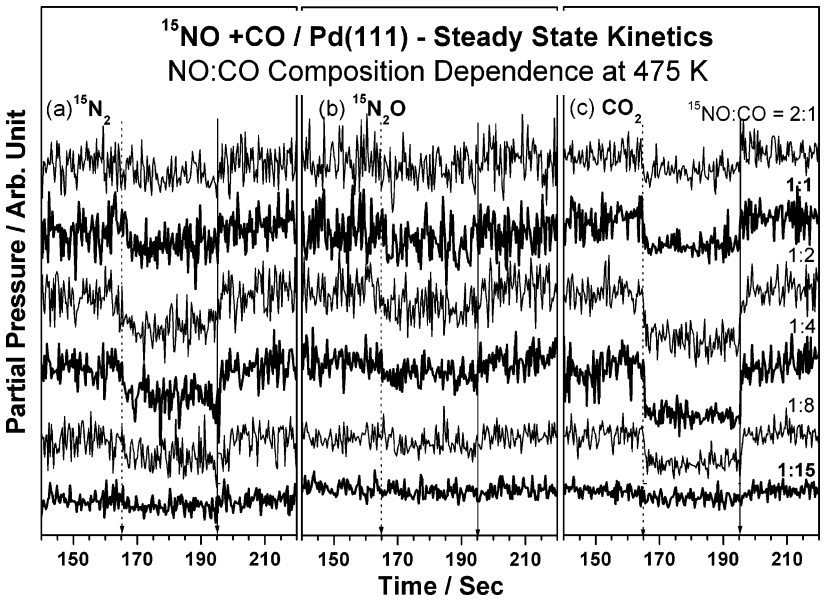

Figure 7. Time evolution of the products (a) N_2, (b) N_2O, and (c) CO_2 for NO:CO beam composition dependent steady-state kinetics at 475 K. Dotted and solid arrows indicate the closing and opening of the shutter.

ment compared to the clean surface. It indicates that some oxygen atoms remain on the surface at the end of the first reaction on clean Pd(111). Furthermore, the restart experiments indicate that the production of N_2 and N_2O does not need any threshold coverage as on Rh(111) surface.[34]

3.3. Steady-State Kinetics. 3.3.1. Temperature Dependence. Figure 6 shows the temperature dependence of molecular beam kinetics in the steady state for the production of N_2, N_2O, and CO_2 for 1:4 NO:CO beam compositions. No NO + CO reaction on Pd(111) could be observed within the detection limits of our experiment up to 425 and $\geq$625 K. The active temperature window for NO reduction lies between 425 and 575 K with a maximum steady-state rate at 475 K. The N_2O production rate is about an order of magnitude lower than that of N_2 production. For $\geq$525 K, the rate slowly decreases and no N_2O production can be observed. The differences in response of the partial pressures of the product species for shutter opening/closing to the new steady state should be noticed, particularly between 475 and 525 K. The partial pressure of CO_2 responds immediately to modulation, whereas the N_2 partial pressures displayed a slow response on beam blocking and unblocking indicating that nitrogen recombination might be the rate-determining step (RDS). However, the low signal-to-noise ratio associated with N_2O makes deriving any meaningful conclusions difficult. However, >525 K, CO_2, and N_2 formation undergo fast changes on beam modulation.

3.3.2. Composition Dependence. Figure 7 shows the dependence of the steady-state kinetics on the NO:CO beam composition at 475 K for compositions ranging from 2:1 to 1:15 of NO:CO. When the beam is rich in NO (for instance, 2:1 NO:CO), the rate of the overall reaction is low compared to other beam compositions even at a high surface temperature. As the beam is made richer in CO, the NO + CO steady-state reaction rate increases until it reaches a maximum of 1:4 NO:CO composition. The N_2O production rate reaches its maximum at the beam composition of 1:2 NO:CO and not for the NO-

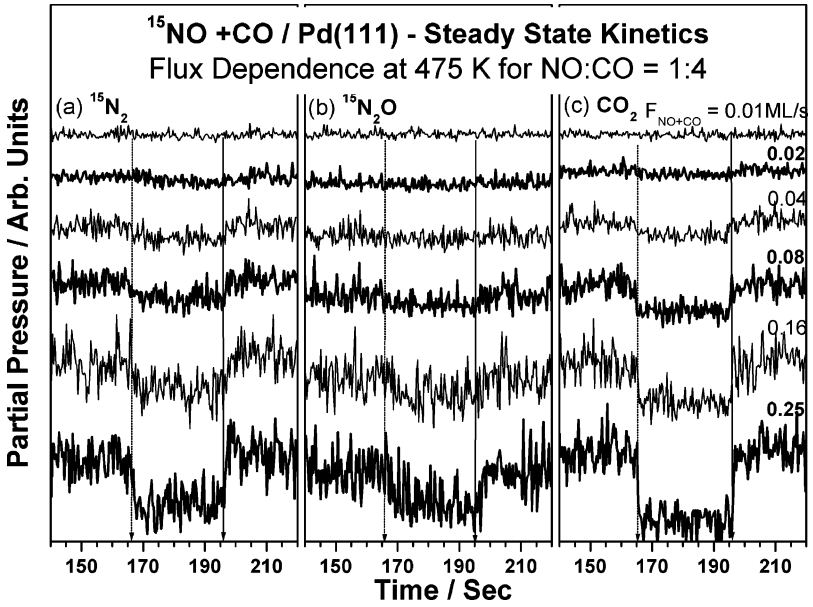

Figure 8. Total beam flux (F_{NO+CO}) dependent steady-state kinetics with a 1:4 NO:CO beam at 475 K for products (a) N_2, (b) N_2O, and (c) CO_2. Dotted and solid arrows indicate the closing and opening of the shutter.

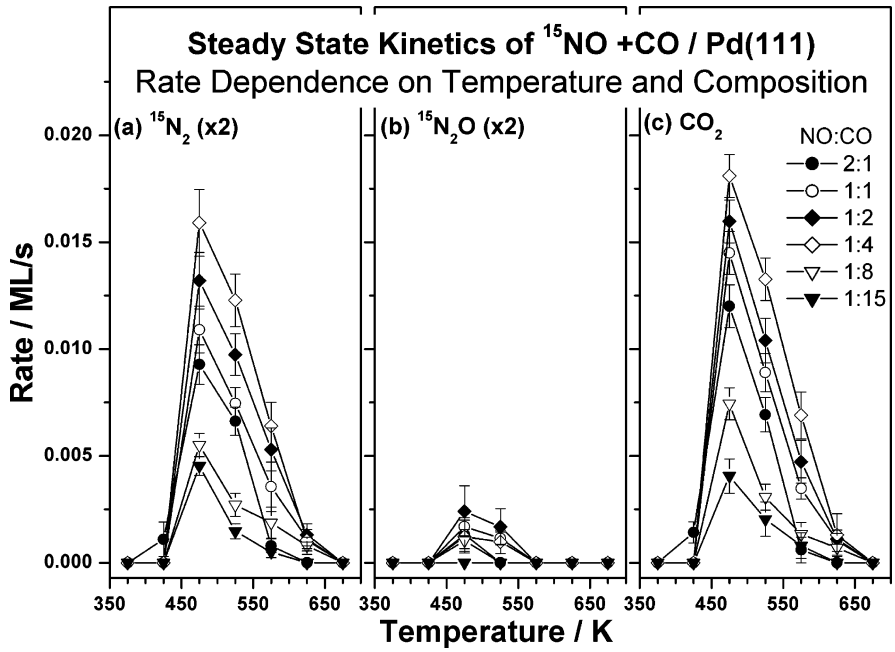

Figure 9. Steady-state rate of production of (a) N_2, (b) N_2O, and (c) CO_2 are given for all NO:CO compositions and reaction temperatures. Maximum rate was observed at 475 K for all NO:CO beam compositions.

rich beams. This clearly indicates that the surface composition established for 1:2 of NO:CO beam composition induces more N_2O production than the NO-rich beam compositions. N_2O production decreases slowly as the beam becomes richer in CO. N_2 and CO_2 production rates decrease on either side of 1:4 NO:CO composition. From Figures 6 and 7, it is observed that the maximum in NO + CO reaction rate occurs at 475 K for the composition of 1:4 NO:CO with a minor production of N_2O.

3.3.3. Flux Dependence. Figure 8 shows the flux dependence of the NO + CO reaction on Pd(111) at 475 K for 1:4 NO:CO for the total fluxes ranging from $F_{NO+CO} = 0.01$ to 0.25 ML/s. The rates of production of the major products N_2 and CO_2 along with N_2O increase linearly with increasing total beam flux and indicate a first order dependence on F_{NO}. The studies on flux dependence clearly show the slow change in the partial pressure of N_2 for beam blocking and unblocking and suggest that nitrogen formation could be the RDS for the NO + CO reaction on Pd(111) surfaces below 500 K and for $F_{NO+CO} \leq 0.16$ ML/s. Further, at a high flux ($F_{NO+CO} = 0.25$ ML/s), N_2 production also shows fast changes on beam blocking and unblocking, suggesting that there may be a contribution from other reaction steps to the RDS as well.

3.4. Steady-State Reaction Rates. Figure 9 shows the rate of formation of all the three products namely, (a) N_2, (b) N_2O, and (c) CO_2 measured in the steady-state at a total flux of 0.25 ML/s. All beam compositions show a reaction maximum at 475 K. At the reaction temperature of 475 K and the 1:4 NO:CO composition, a maximum in productivity is observed for the major products N_2 and CO_2 and the production maximum for N_2O is observed for a 1:2 NO:CO beam. There is a general broadening of the temperature range in which the rate is

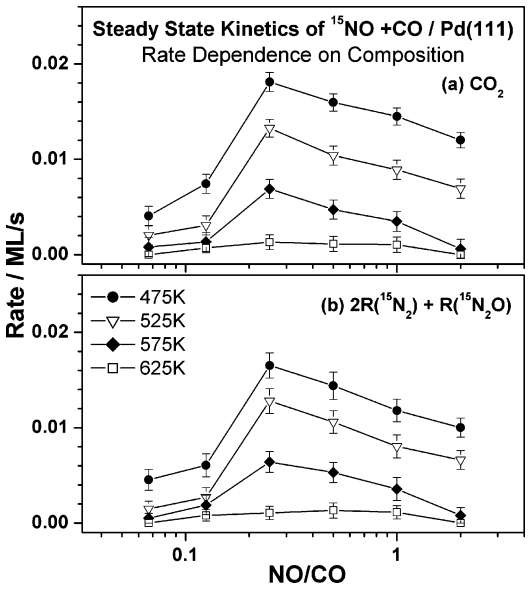

Figure 10. Steady-state rate dependence on the beam composition at four temperatures for (a) CO_2 and (b) $2R(N_2) + R(N_2O)$.

considerable relative to the maximum rate as the beam becomes richer in CO.

The above steady-state rate data is plotted in Figure 10 in a modified and different manner for (a) CO_2 and (b) $2R(N_2) + R(N_2O)$ to clearly see the rate dependence on composition and to see the consistency in the experimental data through eq 1.

$$R(CO_2) = 2R(N_2) + R(N_2O) \quad (1)$$

A good overall correspondence is observed between the rate of CO oxidation and nitrogen containing product formation suggesting that the data is self-consistent within the error limit. This figure also confirms that the maximum in the reaction rate is observed for a NO:CO ratio of 1:4. All the NO:CO compositions shows a reaction maximum at 475 K.

3.5. Temperature-Programmed Desorption (TPD) Studies. TPD experiments were performed to measure the surface nitrogen left after the NO + CO reaction on Pd(111) surface at a heating rate of 5 K/s. Two TPD results recorded after the 1:4 NO:CO reaction at (a) 475 and (b) 525 K are given in Figure 11. Both experiments show nitrogen desorption around 500 K in a single peak. Generally, TPD results from the surfaces that are exposed to a beam of any composition at $T > 525$ K show only low oxygen coverage after the reaction. However, the coverage of oxygen measured through CO-titration varies from one experiment to another. This effect may be attributed to subsurface and bulk diffusion,[35] which makes the reliable estimation of oxygen coverage difficult. At 475 and 525 K, a small coverage of nitrogen is also observed for all beam compositions and θ_N is ≤ 0.05 ML. At lower reaction temperatures (375 and 425 K) the desorption of all the products and reactants is seen. Large amounts of NO (>0.18 ML) or CO (>0.25 ML) are desorbed from surfaces that are exposed to NO-rich (2:1 and 1:1 NO:CO) or CO-rich (1:8 and 1:15 NO:CO) beams at 375 K, respectively, indicating surface poisoning, as observed in the transient coverage results (Figure 3).

4. Discussion

4.1. Reaction Mechanism. The isothermal kinetic data obtained provide some new insights on the mechanism of the NO + CO reaction on Pd surfaces. The following elementary surface reactions are considered for the overall NO + CO reaction on Pd(111) surfaces:

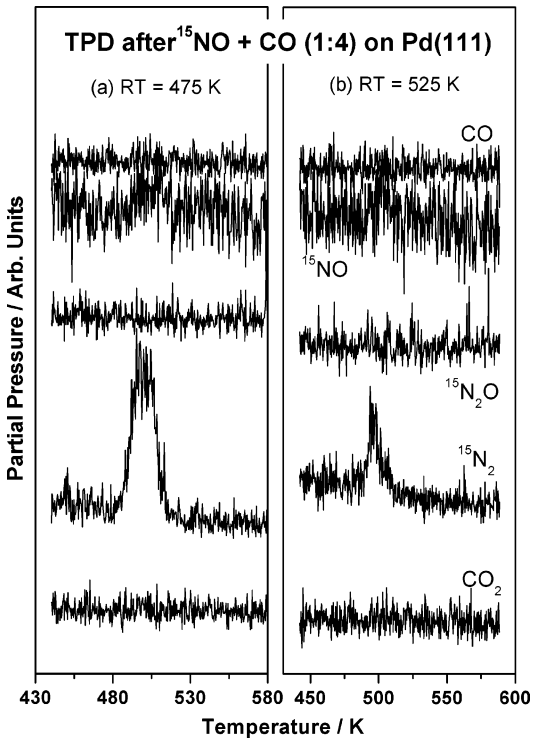

Figure 11. TPD recorded after the NO + CO reaction with 1:4 beam composition at (a) 475 and (b) 525 K. The nitrogen coverage decreases with increasing temperature and no nitrogen coverage is observed at reactions temperatures >525 K.

$$CO_{(g)} \xrightarrow{k_2} CO_{(ads)} \quad (2)$$

$$CO_{(ads)} \xrightarrow{k_3} CO_{(g)} \quad (3)$$

$$NO_{(g)} \xrightarrow{k_4} NO_{(ads)} \quad (4)$$

$$NO_{(ads)} \xrightarrow{k_5} NO_{(g)} \quad (5)$$

$$NO_{(ads)} \xrightarrow{k_6} N_{(ads)} + O_{(ads)} \quad (6)$$

$$CO_{(ads)} + O_{(ads)} \xrightarrow{k_7} CO_{2(g)} \quad (7)$$

$$N_{(ads)} + N_{(ads)} \xrightarrow{k_8} N_{2(g)} \quad (8)$$

$$N_{(ads)} + NO_{(ads)} \xrightarrow{k_9} N_2O_{(g)} \quad (9)$$

The overall reaction is

$$(x+y)NO + xCO \xrightarrow{k_{10}} \left(\frac{x-y}{2}\right)N_2 + xCO_2 + yN_2O \quad (10)$$

One of the important controversies in the literature with respect to the NO + CO reaction mechanism relates to the reaction RDS.[20,25] Our kinetic results clearly show that the CO_2 production is fast compared to N_2 and/or N_2O production under the present experimental conditions. This also suggests that the NO adsorption and its dissociation cannot be the RDS, at least in the low-temperature regime, <525 K. This leaves eq 8 or 9 to be a possible RDS. The low signal-to-noise ratio associated with N_2O makes deriving any meaningful conclusions difficult. Further, N_2O being a minor product in the parallel pathway for

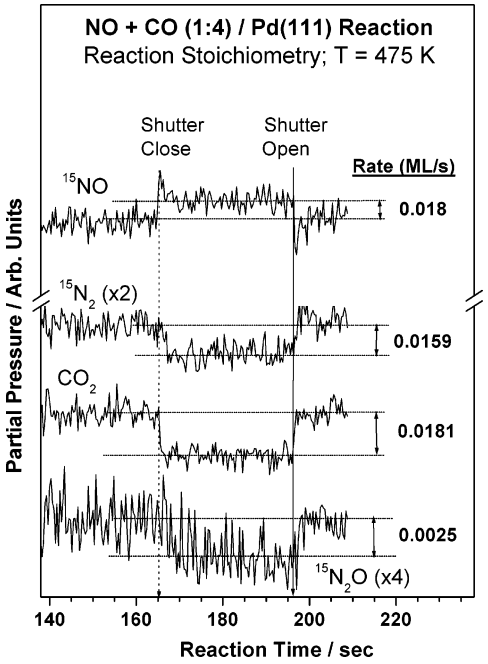

Figure 12. Steady-state reaction rates for the NO uptake and N_2, N_2O, and CO_2 production at 475 K with 1:4 NO:CO beam on the Pd(111) surface. The absolute values of the rate were calculated and given for NO and all the products. It is to be noted that the stoichiometry observed in all the experiments changes at temperatures above 525 K, as there is no N_2O production and a 1:1 ratio of CO_2:$^1/_2N_2$ is observed.

both N_2 and N_2O formation, it is ruled out that N_2O formation can be the RDS. A slow change in partial pressure of N_2 was observed below 525 K for the beam blocking in the steady-state of NO + CO reactions under most of the conditions; however, high flux (F_{NO+CO} = 0.25 ML/s) measurements (Figure 8) shows the fast changes in N_2 production for beam blocking. It is likely that also the other steps (in particular NO dissociation) have some degree of rate control <525 K (as indicated by the linear flux dependence of the reaction rate in Figure 8). This suggests that the N_2 formation from the recombination of N atoms below 525 K might be controlling the overall reaction; however the NO dissociation also have some degree of rate control as indicated above. Above 525 K, CO_2 as well as N_2 formation shows fast changes for beam blocking and unblocking. Furthermore, the rate of desorption of reactants species is faster than the adsorption and NO dissociation, and hence, a decrease in overall NO + CO rate for >525 K is observed. In the high-temperature regime, it is expected that the degree of rate control by NO dissociation increases and the degree of rate control of the other steps decreases.

Another piece of evidence to support the reaction mechanism suggested above, as well as to calculate the reaction stoichiometry, is given in Figure 12. The rate of adsorption of NO and the rate of formation of various products in the steady-state is shown for 1:4 NO:CO beam composition at a surface temperature of 475 K in Figure 12. It is to be noted that the rate of NO adsorption (0.018 ML/s) in the steady state is equal to that of the sum of either CO_2 (0.0181 ML/s) and N_2O production (0.0006 ML/s) or $2N_2$ (0.016 ML/s) and $2N_2O$ (0.0012 ML/s) production, within the error limit (10%). The above result suggests that about 90% of adsorbed NO dissociates and the remaining amount is adsorbed in the molecular state. At temperatures higher than 525 K, a ratio of 1:1 for CO_2:$^1/_2N_2$ is observed suggests that the rate of NO-uptake is equal to that of CO_2 or $^1/_2N_2$ production. The above two stoichiometries, below and above 525 K, were found to hold good for all the reaction conditions employed in our experiments.

4.2. Steady-State Kinetics. Under steady-state conditions, the rate of all the elementary processes should be equal. However, the recombination of N + N is considered as the RDS due to the low rate constant values. Alternatively, the rates of other elementary processes compensate under steady-state conditions through changes in the respective surface coverage.[36] From the above discussion and the arguments of section 4.1, the rate expression for CO_2 is derived from the surface coverage of the different adsorbates.

$$R(CO_2) = k_7\theta_{CO}\theta_O \tag{11}$$

It is clear that the oxygen for CO oxidation is provided exclusively by NO dissociation, and hence, θ_O entirely depends on eq 6. It is also well-known that k_7 is a function of surface coverages. Furthermore, θ_O and $R(CO_2)$ also depend on the F_{NO} as given in eqs 12 and 13:

$$\theta_O = \frac{k_6}{k_7}\frac{\theta_{NO}\theta_{vac}}{\theta_{CO}} = \frac{k_6\theta_{vac}}{k_7}\frac{s^0_{NO}}{k_5 + k_6\theta_{vac}}\frac{\theta_{vac}}{\theta_{CO}}F_{NO} \tag{12}$$

and hence

$$R(CO_2) = \frac{k_6}{k_5 + k_6\theta_{vac}}\theta_{vac}{}^2 s^0_{NO}F_{NO} \tag{13}$$

The s_{NO} changes with temperature and the surface coverage and hence the number of vacant sites too. This also directly affects the proportionality in eq 13. Nitrogen atoms also desorb as N_2 around 500 K creating more vacant sites. This hints at a high rate constant for CO_2 production and hence fast changes in the steady-state kinetics.

The CO molecules in the 1:2 and 1:4 of NO:CO compositions remove the dissociated O atoms effectively from the surfaces, especially around 500 K, thereby increasing the reaction rate and the number of vacant sites. This helps in turn a larger dissociation of NO. However, at >500 K, s_{NO} and s_{CO} decrease very much and lead to a number of vacant sites; NO and CO desorption rates may play a significant role increasingly at higher temperatures.[23−25]

In the CO-rich beam (1:15 of NO:CO) the NO + CO reaction is not effective under the present experimental conditions. This is attributed to a CO poisoning effect at <500 K and fast desorption of NO at >500 K. Contrarily, in NO-rich beams (2:1 NO:CO) the dissociated O and N atoms hinder the further adsorption of reactants in the steady state by occupying the sites. CO displacement by NO also leads to a low θ_{CO} and hence a low overall rate. No reactivity is observed at >625 K on Pd-(111), compared to the reported reactivity of NO + CO reaction on powder and model supported Pd-catalysts.[20,23] Henry et al.[23] invoked the reverse spillover effect from the support to the metal on Pd/MgO, which helps to move NO_{ads}/MgO to Pd and cause its dissociation at temperatures as high as 723 K and sustain the NO + CO reaction. This explains the high-temperature activity of Pd for the NO + CO reaction and its application in TWC.

Present TPD measurements after the reaction at temperatures ≥525 K reveal no θ_N and/or θ_{NO} on Pd(111) and indicates that no stabilized NO molecules are present, in contradiction to ref 20. Adsorption of NO/Pd(111)[31] also shows no stabilized N adatoms and/or NO molecules and generally our results are in agreement with the TPD data reported by several groups.[13,22,28−30] Besides, a plot of the steady-state rate as a function of

temperature on Pd/MgO[23] displays a volcano shape with a rate maximum between 475 and 525 K, which is in good agreement with the present results. However, a linear increase in rate with temperature up to 625 K on Pd(111) by Goodman et al.[20] is considerably different from our present results. It should be pointed out that reasons for the above discrepancy could be due to the differences between the present single scattering molecular beam experiments, and the batch mode reaction at high pressure ($P_{NO} = P_{CO} = 1$ Torr) employed to measure the rate by Goodman et al.[20] Batch reactor studies at high pressure cannot be directly comparable. Furthermore, the reaction mechanism at >500 K is also considerably different at high pressure and under UHV conditions. At high pressure, high θ_{NO} observed leads to more N_2O;[20,21] however, only N_2 was produced under UHV conditions in the present report and by Henry et al.[23,25]

4.3. A Comparison between (NO + CO)/Pd(111) and (NO + CO)/Rh(111). Rh surfaces show high catalytic activity for NO reduction,[1−3] and the NO + CO reaction on Rh(111) has been studied in detail by Zaera et al.,[34,36−40] and Belton et al.[41] It is now worth comparing the activity of Pd(111) and Rh(111) for the NO + CO reaction. The important similarities and differences between the present results on (NO + CO)/Pd(111) obtained using a molecular beam setup and those reports on Rh(111)[34,36−38] are presented briefly below. The isothermal kinetic data presented in this work shows a significant reactivity on Pd(111) compared to Rh(111) for the NO + CO reaction.[34,36−38] A comparable catalytic activity of Pd(111) to the (NO + CO)/Rh(111) system[36] was observed in the steady state; however, only in the temperature window 425−575 K. However, Rh(111) is active in a wider temperature range from 450 to 900 K.[36] A considerable amount of N_2O production is directly observed on Pd(111) system, but no N_2O was observed directly on Rh(111) under UHV conditions.

The production of N_2 in the transient state is instantaneous on Pd(111) system; however, on Rh(111) system,[34,36−38] N_2 production starts only after the accumulation of a threshold coverage of adsorbed nitrogen on the surface which depends on the beam composition and surface temperature. On the basis of the spontaneity of N_2 production, it is clear that no threshold nitrogen coverage concept is operating on the Pd(111) system. At the same time in the (NO + CO)/Rh(111) system, CO_2 and N_2 are produced rapidly in the transient state at low (450−550 K) and high temperatures (>550 K), respectively, because of the immediate availability of surface oxygen or nitrogen atoms from the fast NO dissociation step.[34] This is mainly attributed to the relatively large and constant s_{NO} (∼0.8)[39] on Rh(111). The value of s_{NO} is less than 0.5 above 400 K on Pd(111), and this limits the reaction to a large extent and a trend similar to that of Rh(111) is not observed. Additionally, the displacement of CO by NO was observed in the temperature range of 375−475 K in the transient state indicating that the lateral repulsive interactions of CO are more than NO[20] at least above 375 K. The occurrence of a similar displacement effect on Rh(111) system has also been demonstrated.[34]

Although not discussed due to the lack of direct evidence, the nitrogen formation through N_2O intermediate is not ruled out on Pd(111). However, Zaera and Gopinath[40] have published kinetic evidence for the formation of nitrogen through an N_2O intermediate on Rh(111). Loffreda et al.,[17−19] have investigated the NO + CO reaction through theoretical calculations on (111) and (100) facets of Pd and Rh surfaces and found that NO dissociation was endothermic on Pd and exothermic on Rh at low coverages. In general, the above comparison indicates a good similarity in the activities of Pd and Rh, and more work needs to be carried out for full commercial exploitation of Pd.

5. Conclusions

A kinetic study on the NO + CO reaction on Pd(111) surfaces carried out at a wide range of temperature, beam composition and total flux is reported. The isothermal kinetic study of the NO + CO reaction on Pd(111) surfaces reveals significant and comparable catalytic activity as that of Rh(111) in the narrow temperature window 475−575 K. Detailed kinetic experiments and analysis suggests that N_2 formation limits the rate of the overall reaction below 525 K. However, the NO dissociation step contributes in a major way toward the RDS above 525 K. Direct displacement of CO_{ads} by NO was observed between 375 and 475 K and the transient state coverage calculations show that the surface composition was different from the NO:CO beam composition at low temperatures. The rate of NO + CO reaction increases linearly with increasing total beam flux and indicates a first order dependence on F_{NO}.

Irrespective of the NO:CO composition, a rate maximum always occurs at 475 K (or between 475 and 525 K) for all the beam compositions investigated. However, there is a broadening of the active rate regime from 475 to 525 K for 2:1 to 475−625 K for 1:4 NO:CO. The reaction rate is maximum for the 1:4 NO:CO beam composition among all the compositions studied. Both NO-rich and CO-rich beams show poor catalytic activity and is attributed to surface poisoning by those species.

Acknowledgment. The authors are grateful to Professor H.-J. Freund, FHI, Berlin, for his keen interest and support for the present work. C.S.G. thanks Dr. B. D. Kulkarni, NCL, for noise reduction analysis of our data and helpful discussions. Financial support for this project by the Volkswagen Foundation (Program of Partnership, "The Mechanism and Kinetics of NO Reduction Reactions on Noble Metal Surfaces—From Single Crystal Surfaces to Supported Model Catalysts") is gratefully acknowledged. C.S.G. thanks the Alexander von Humboldt (AvH) foundation for a grant used to build part of the molecular beam facility at NCL under the instrument donation program to the former AvH fellows. C.S.G. also thanks NCL, Pune, India, for an in-house project (MLP004226). K.T. thanks the CSIR, New Delhi, for a senior research fellowship.

References and Notes

(1) Taylor, K. C. *Catal. Rev. Sci. Eng.* **1993**, *35*, 457.
(2) Shelef, M.; Graham, G. W. *Catal. Rev. Sci. Eng.* **1994**, *36*, 433.
(3) Zhdanov, V. P.; Kasemo, B. *Surf. Sci. Rep.* **1997**, *29*, 31.
(4) Kreuzer, T.; Lox, S. E.; Lindner, D.; Leyrer, J. *Catal. Today* **1996**, *29*, 17 and references therein.
(5) van Yperen, R.; Lindner, D.; Mu*β*mann, L.; Lox, E. S.; Kreuzer, T. *Stud. Surf. Sci. Catal.* **1998**, *116*, 51.
(6) Tagliaferri, S.; Köppel, R. A.; Baiker, A. *Stud. Surf. Sci. Catal.* **1998**, *116*, 61.
(7) Takahashi, N.; Shinjoh, H.; Iijima, T.; Suzuki, T.; Yamazaki, K.; Yokota, K.; Suzuki, H.; Miyoshi, N.; Matsumoto, S.; Tanizawa, T.; Tanaka, T.; Tateishi, S.; Kasahara, K. *Catal. Today* **1996**, *27*, 63.
(8) Fridell, E.; Persson, H.; Olsson, L.; Westerberg, B.; Amberntsson, A.; Skoglundh, M. *Top. Catal.* **2001**, *16*, 133.
(9) Berndt, H.; Schutze, F. W.; Richter, M.; Sowade, T.; Grunert, W. *Appl. Catal., B* **2003**, *40*, 51.
(10) Jobson, E. *Top. Catal.* **2004**, *28*, 191.
(11) Johánek, V.; Schauermann, S.; Laurin, M.; Gopinath, C. S.; Libuda, J.; Freund, H.-J. *J. Phys. Chem. B* **2004**, *108*, 14244.
(12) Johánek, V.; Schauermann, S.; Laurin, M.; Libuda, J.; Freund, H.-J. *Angew. Chem., Inter. Ed.* **2003**, *42*, 3035.
(13) de Wolf, C. A.; Nieuwenhuys, B. E. *Surf. Sci.* **2000**, *469*, 196.
(14) Hammer, B. *J. Catal.* **2001**, *199*, 171.
(15) Hirisimäki, M.; Valden, M. *J. Chem. Phys.* **2001**, *114*, 2345.
(16) Bowker, M.; Bennett, R. A.; Jones, I. Z. *Top. Catal.* **2004**, *28*, 25.
(17) Loffreda, D.; Simon, D.; Sautet, P. *J. Chem. Phys.* **1998**, *108*, 6447.

(18) Loffreda, D.; Simon, D.; Sautet, P. *Chem. Phys. Lett.* **1998**, *291*, 15.
(19) Loffreda, D.; Simon, D.; Sautet, P. *J. Catal.* **2003**, *213*, 211.
(20) Rainer, D. R.; Vesecky, S. M.; Koranne, M.; Oh, W. S.; Goodman, D. W. *J. Catal.* **1997**, *167*, 234 and references therein.
(21) Ozensoy, E.; Goodman, D. W. *Phys. Chem. Chem. Phys.* **2004**, *6*, 3765, and references therein.
(22) Nakamura, I.; Fujitani, T.; Hamada, H. *Surf. Sci.* **2002**, *514*, 409.
(23) Piccolo, L.; Henry, C. R. *Appl. Surf. Sci.* **2000**, *162*−*163*, 670.
(24) Piccolo, L.; Henry, C. R. *J. Mol. Catal. A* **2001**, *167*, 181.
(25) Prévot, G.; Henry, C. R. *J. Phys. Chem. B* **2002**, *106*, 12191. Prevot, G.; Meerson, O.; Piccolo, L.; Henry, C. R. *J. Phys. Condens. Matt.* **2002**, *14*, 4251.
(26) Sharpe, R. G.; Bowker, M. *Surf. Sci.* **1996**, *360*, 21.
(27) Burghaus, U.; Jones, I. Z.; Bowker, M. *Surf. Sci.* **2000**, *454*−*456*, 326.
(28) Ramsier, R. D.; Gao, Q.; Waltenburg, H. N.; Yates, J. T., Jr. *J. Chem. Phys.* **1994**, *100*, 6837.
(29) Bertolo, M.; Jacobi, K.; Nettesheim, S.; Wolf, M.; Hasselbrink, E. *Vacuum* **1990**, 76.
(30) Bertolo, M.; Jacobi, K. *Surf. Sci.* **1990**, *226*, 207.
(31) Thirunavukkarasu, K.; Thirumoorthy, K.; Libuda, J.; Gopinath, C. S. *J. Phys. Chem. B* **2005**, *109*, 13283.
(32) Haq, S.; Hodgson, A. *Surf. Sci.*. **2000**, *463*, 1.
(33) Stacchiola, D.; Thompson, A. W.; Kaltchev, M.; Tysoe, W. T. *J. Vac. Sci. Technol. A* **2002**, *20*, 2101.
(34) Gopinath, C. S.; Zaera, F. *J. Phys. Chem. B* **2000**, *104*, 3194.
(35) Leisenberger, F. P.; Koller, G.; Sock, M.; Surnev, S.; Ramsey, M. G.; Netzer, F. P.; Klötzer, B.; Hayek, K. *Surf. Sci.* **2000**, *445*, 380.
(36) Gopinath, C. S.; Zaera, F. *J. Catal.* **1999**, *186*, 387.
(37) Zaera, F.; Gopinath, C. S. *J. Chem. Phys.* **1999**, *111*, 8088.
(38) Gopinath, C. S.; Zaera, F. *J. Catal.* **2001**, *200*, 270.
(39) Aryafar, M.; Zaera, F. *J. Catal.* **1998**, *175*, 316.
(40) Zaera, F.; Gopinath, C. S. *Chem. Phys. Lett.* **2000**, *332*, 209.
(41) Belton, D. N.; Schmieg, S. J. *J. Catal.* **1993**, *144*, 9. Ng, K. Y. S.; Belton, D. N.; Schmieg, S. J.; Fisher, G. B. *J. Catal.* **1994**, *146*, 394. Peden, C. H. F.; Belton, D. N.; Schmieg, S. J. *J. Catal.* **1995**, *155*, 204.